



HAL
open science

Increasing the dilution rate can globally stabilize two-step biological systems

Jérôme Harmand, Alain Rapaport, Denis Dochain

► **To cite this version:**

Jérôme Harmand, Alain Rapaport, Denis Dochain. Increasing the dilution rate can globally stabilize two-step biological systems. *Journal of Process Control*, 2020, 95, pp.67-74. 10.1016/j.jprocont.2020.08.009 . hal-02926040v1

HAL Id: hal-02926040

<https://hal.inrae.fr/hal-02926040v1>

Submitted on 31 Aug 2020 (v1), last revised 1 Oct 2020 (v2)

HAL is a multi-disciplinary open access archive for the deposit and dissemination of scientific research documents, whether they are published or not. The documents may come from teaching and research institutions in France or abroad, or from public or private research centers.

L'archive ouverte pluridisciplinaire **HAL**, est destinée au dépôt et à la diffusion de documents scientifiques de niveau recherche, publiés ou non, émanant des établissements d'enseignement et de recherche français ou étrangers, des laboratoires publics ou privés.



Distributed under a Creative Commons Attribution - NonCommercial - NoDerivatives 4.0
International License

Increasing the dilution rate can globally stabilize two-step biological systems

J. Harmand ^{a,*} A. Rapaport ^b D. Dochain ^c

^a*INRAE, Univ Montpellier, LBE, 102 avenue des Etangs, 11100, Narbonne, France.*

^b*INRAE, Univ. Montpellier, MISTEA, Montpellier SupAgro, France.*

^c*ICTEAM, Univ. Cath. Louvain, Belgium.*

Abstract

We revisit two-step mass-balance models of biological processes as met to describe numerous biological systems including the anaerobic digestion or the nitrification process in view of its global stabilization. We show that when a bi-stability occurs, it can be possible to globally stabilize the dynamics toward an unique positive equilibrium by increasing the dilution rate. We give sufficient conditions on the growth functions of the model for this situation to appear. This illustrates that for biological multi-step reactional systems, increasing the residence time (*e.g.* decreasing the input flow rate) may not be the only way to stabilize the dynamics.

Key words: Anaerobic digestion, nitrification, chemostat, multi-stability, stabilization.

1 Introduction

In most of continuous cultures, it is well known that increasing the dilution rate (or equivalently reducing the residence time inside the reactors) can destabilize the dynamics, in the sense that it enlarges the attraction basin of the wash-out equilibrium. This can be easily shown on the classical mathematical model of the chemostat, whatever the kinetics includes inhibition or not (see [6]). For growth inhibited by the substrate, bi-stability systematically occurs

* Corresponding author.

Email addresses: `jerome.harmand@inrae.fr` (J. Harmand),
`alain.rapaport@inrae.fr` (A. Rapaport), `denis.dochain@uclouvain.be`
(D. Dochain).

for large values of the input concentration of substrate. This feature has practical impacts on positive equilibrium (when it exists) because it cannot be globally stable, and the dynamics can conduct the system to the wash-out of the biomass, when the state belongs to the attraction basin of the washout equilibrium. Ways to guarantee a global stability is either to fix a lower dilution rate, which is penalizing for the performance of the process, or to control the dilution rate with a feedback loop, which temporarily diminishes the dilution rate when the state is far from the positive steady state [1, 8, 9, 17]. In any case, the removal has to be reduced at a certain stage.

Here we consider a more complex reaction scheme that are two-step systems, as met for instance in many models representing the anaerobic digestion process [4] or the nitrification process [20]. For these systems we show that there exist situations presenting a bi-stability for which increasing (and not decreasing) the dilution rate also leads the system to a globally asymptotically stable steady state, in opposition to classical stabilizing practices. In such a way, we can treat more matter per unit time during the transient than when decreasing the dilution rate.

In the paper, we denote by \mathbb{R}_+ the set of non-negative numbers and by $\mathbb{R}_{+,*}$ the set of positive numbers.

Let us consider the general mathematical model of a two-step mass-balance biological process, given by the following equations:

$$\begin{cases} \dot{x}_1 = \mu_1(s_1)x_1 - \alpha Dx_1 \\ \dot{s}_1 = -\mu_1(s_1)x_1 + D(s_1^{in} - s_1) \\ \dot{x}_2 = \mu_2(s_2)x_2 - \alpha Dx_2 \\ \dot{s}_2 = -\mu_2(s_2)x_2 + \mu_1(s_1)x_1 + D(s_2^{in} - s_2) \end{cases} \quad (1)$$

where the parameter D denotes the dilution rate.

This model is presented under the original form proposed in [4]. The first reaction involves a microbial species of concentration x_1 which grows on a substrate of concentration s_1 with a monotonic specific rate μ_1 . The incoming flow fed the culture with substrate of concentration s_1^{in} . The second reaction involves a second microbial species of concentration x_2 which grows on another substrate of concentration s_2 , with a specific growth rate denotes μ_2 . This reaction is also fed by the first one which produces the second substrate. In addition, the incoming flow rate may contain (or not) substrate of concentration s_2^{in} . The parameter $\alpha \in (0, 1]$ reflects the fact that the effective dilution rate of the biomass is impacted by a retention inside the tank, differently to the abiotic resource. Here, the yield coefficients of the transformations of substrate s_i into biomass x_i ($i = 1, 2$), and of the production of substrate for the

second reaction by the first one, have been all kept equal to 1 (this is always possible without any loss of generality, by a right choice of the concentration units).

In many biological systems, such as the anaerobic digestion or the nitrification processes, it is often reported in the literature that the second reaction is inhibited by large values of s_2 , which amounts to consider the following hypotheses.

Assumption 1 *The functions μ_1, μ_2 belong to $C^1(\mathbb{R}_+, \mathbb{R}_+)$ and fulfill the following properties.*

- (i) μ_1 is increasing on \mathbb{R}_+ with $\mu_1(0) = 0$.
- (ii) There exists $\hat{s}_2 > 0$ such that μ_2 is increasing on $[0, \hat{s}_2)$ and decreasing on $(\hat{s}_2, +\infty)$, with $\mu_2(0) = 0$ and $\mu_2(+\infty) = 0$.

The model (1) has a cascade structure: the first reaction is independent of the second one and the (x_1, s_1) sub-system follows the classical (mono-specific) chemostat model. However, the (x_2, s_2) sub-system is more complex to study as it receives substrate from the first reaction and μ_2 is non-monotonic. This model and some of its variants has been already well studied in the literature [3, 4, 14], depending on the operating parameters (s_1^{in}, s_2^{in}, D) . In particular, it has been shown that the dynamics may exhibit a multiple-stability, and the complete operating diagram has been established in [15, 20]. The purpose of the present work is to complement those studies, investigating how to adapt the value of the dilution rate D to ensure a global stability of the dynamics. For sake of completeness, we first recall in the next section the set of possible asymptotic behaviors of the model.

2 Stability analysis

Let us first denote, for convenience,

$$\mu_1^m := \sup\{\mu_1(s_1) ; s_1 \in \mathbb{R}_+\}, \quad \mu_2^m := \sup\{\mu_2(s_2) ; s_2 \in \mathbb{R}_+\} = \mu_2(\hat{s}_2).$$

We define the break-even concentration λ_1 associated to the first reaction as the function

$$\lambda_1(D) := \mu_1^{-1}(\alpha D), \quad \alpha D < \mu_1^m. \quad (2)$$

Then, we define the following quantity

$$\overline{s_2^{in}}(D) := s_2^{in} + \begin{cases} s_1^{in} - \lambda_1(D), & \alpha D < \mu_1(s_1^{in}) \\ 0, & \alpha D \geq \mu_1(s_1^{in}) \end{cases} \quad (3)$$

that is playing an important role in the analysis of the equilibria, as an "effective" input concentration for the second reaction.

As plotted in Figure 1, we define also the break-even concentrations λ_2^-, λ_2^+ associated to the second reaction as functions such that

$$[\lambda_2^-(D), \lambda_2^+(D)] := \{s_2 \in \mathbb{R}_+; \mu_2(s_2) \geq \alpha D\}, \quad \alpha D \leq \mu_2^m. \quad (4)$$

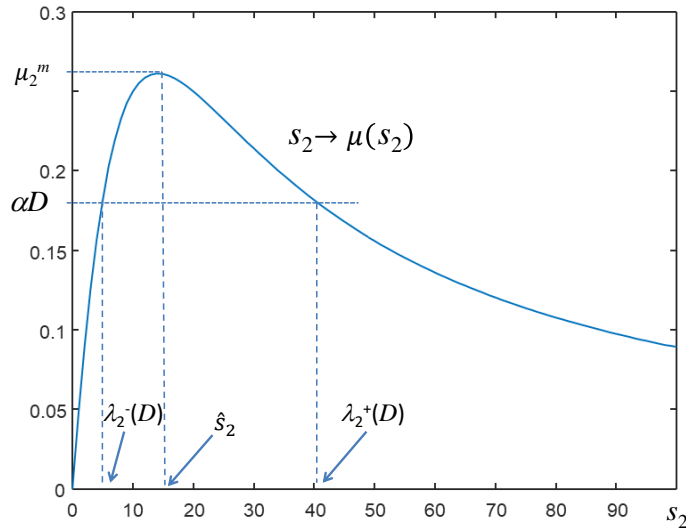


Fig. 1. Definition of $\lambda_2^-(D)$ and $\lambda_2^+(D)$

These numbers represent thresholds on the substrate concentration for which a microbial species cannot survive outside the interval of values delimited by these numbers, because their growth is not high enough to compensate the dilution rate. This limiting values are often called 'break-even concentrations' in the microbial ecology literature (see for instance [10]).

One has the following result about equilibria of system (1) and their stability.

Proposition 1 *The asymptotic behavior of the solutions of system (1) with initial condition in $(\mathbb{R}_{+*} \times \mathbb{R}_+)^2$ is given by one of the following cases.*

- (1) *When $\alpha D > \max(\mu_1(s_1^{in}), \mu_2^m)$, any solution converges to the "double wash-out" steady-state $E^{0,0} := (0, s_1^{in}, 0, s_1^{in})$.*

- (2) When $\max(\mu_1(s_1^{in}), \mu_2(s_2^{in})) \leq \alpha D \leq \mu_2^m$, the solution converges either to $E^{0,0}$ or to the equilibrium $E^{0,*} := (0, s_1^{in}, (s_2^{in} - \lambda_2^-(D))/\alpha, \lambda_2^-(D))$, except for initial conditions on a set of null measure
- (3) When $\mu_1(s_1^{in}) < \alpha D \leq \mu_2^m$ and $s_2^{in} \leq \lambda_2^+(D)$, any solution converges to $E^{0,*}$.
- (4) When $\mu_1(s_1^{in}) > \alpha D > \mu_2(s_2)$ for any $s_2 < \overline{s_2^{in}}(D)$, any solution converges to $E^{*,0} := ((s_1^{in} - \lambda_1(D))/\alpha, \lambda_1(D), 0, \overline{s_2^{in}}(D))$.
- (5) When $\alpha D < \mu_1(s_1^{in})$, $\alpha D \leq \mu_2^m$ and $\overline{s_2^{in}}(D) > \lambda_2^+(D)$, the solution converges either to $E^{*,0}$ or to the positive equilibrium $E^{*,*} := ((s_1^{in} - \lambda_1(D))/\alpha, \lambda_1(D), (\overline{s_2^{in}}(D) - \lambda_2^-(D))/\alpha, \lambda_2^-(D))$, except for initial conditions on a set of null measure.
- (6) When $\alpha D < \mu_1(s_1^{in})$, $\alpha D \leq \mu_2^m$ and $\lambda_2^-(D) < \overline{s_2^{in}}(D) \leq \lambda_2^+(D)$, any solution converges to $E^{*,*}$.

This result has already been proved in [3, 4, 14], and we recall quickly here the arguments of the proof based on the study of the single chemostat model, for which the classical results are recalled in the appendix. Let us stress that the statement of Proposition 1 does not distinguish the number of unstable equilibria nor the hyperbolic characteristics of the equilibria, differently to [3]. Our goal here is simply to characterize the possible asymptotic behaviors towards a stable equilibrium, up to a set of initial conditions of null measure.

PROOF. Let us first note that one has $\dot{x}_1 = 0$ when $x_1 = 0$, and $\dot{x}_2 = 0$ when $x_2 = 0$. By uniqueness of the solutions of the system of differential equations (1), we deduce that the solutions verify $x_1(t) > 0$, $x_2(t) > 0$ for any $t > 0$. At $s_1 = 0$ and $s_2 = 0$, one has $\dot{s}_1 = Ds_1^{in} > 0$ and $\dot{s}_2 > Ds_2^{in} > 0$, which shows that the hyperplanes $s_1 = 0$, $s_2 = 0$ are repulsive. We deduce that the solutions verify $s_1(t) > 0$, $s_2(t) > 0$ for any $t > 0$. This shows that a wash-out of species 1 or both species cannot be reached in finite time.

Consider the variables $z_1 = x_1 + s_1$ and $z_2 = s_1 + x_2 + s_2$. From equations (1), one obtains

$$\dot{z}_1 \leq D(s_1^{in} - \alpha z_1), \quad \dot{z}_2 \leq D(s_1^{in} + s_2^{in} - \alpha z_2)$$

from which one deduces that z_1 and z_2 are bounded. This shows that the non-negative solutions of (1) are bounded.

The (x_1, s_1) dynamics is independent of the variables x_2, s_2 and follows the classical chemostat model with monotonic growth function, whose steady state analysis is recalled in the Appendix (Proposition 4). Two cases are distinguished:

- case A: $\alpha D \geq \mu_1(s_1^{in})$: any solution of the (x_1, s_1) sub-system converges to the wash-out state $E_1^0 := (0, s_1^{in})$.
- case B: $\alpha D < \mu_1(s_1^{in})$: any solution of the (x_1, s_1) sub-system with $x_1(0) > 0$ converges to the positive state $E_1^* := ((s_1^{in} - \lambda_1(D))/\alpha, \lambda_1(D))$.

Then, the cascade structure of the dynamics (1), along with the boundedness of its solutions and the asymptotic behavior of the (x_1, s_1) sub-system allows to proceed with the stability analysis of the system on the reduced dynamics of the (x_2, s_2) subsystem:

$$\begin{cases} \dot{x}_2 = \mu_2(s_2)x_2 - \alpha D x_2 \\ \dot{s}_2 = -\mu_2(s_2)x_2 + \mu_1(s_1^{eq})x_1^{eq} + D(s_2^{in} - s_2) \end{cases} \quad (5)$$

where (x_1^{eq}, s_1^{eq}) is the steady state of the (x_1, s_1) sub-system (*i.e.* E_1^0 or E_1^* when it exists, according to Proposition 4).

In case A, the subsystem (5) is the classical chemostat model with non-monotonic growth, whose steady state analysis is recalled in Proposition 5 (see Appendix). Three cases are then possible depending on the value of αD with respect to μ_2^m and $\mu_2(s_2^{in})$, which are exactly the cases (1), (2), (3) given of the Proposition statement.

In case B, notice that one has $\mu_1(s_1^{eq})x_1^{eq} = D(s_1^{in} - \lambda_1(D))$ which allows to rewrite the reduced (x_2, s_2) dynamics as

$$\begin{cases} \dot{x}_2 = \mu_2(s_2)x_2 - \alpha D x_2 \\ \dot{s}_2 = -\mu_2(s_2)x_2 + D(\overline{s_2^{in}}(D) - s_2) \end{cases} \quad (6)$$

where $\overline{s_2^{in}}(D)$ is defined in (3). This is again the classical chemostat model but with non-monotonic growth and the effective input concentration $\overline{s_2^{in}}(D)$, for which the steady state analysis given in Proposition 5 of the Appendix applies. This gives straightforwardly the cases (4), (5), (6) of the statement. \square

In practice, only case (6) is desirable because it guarantees that in any situation the wash-out of both species is avoided. Usually, the dilution rate D is the operating parameter that can be easily manipulated. In the next section, we study how to change the value of D to be in case (6) when the original operating conditions are not in this case.

3 Wash-out avoidance

In this section, we consider situations for which the attraction basin of equilibria with wash-out of biomass 1 or 2 or both is non empty. According to Proposition 1, this happens in cases (1) to (5). We study now how to play only with the value of the dilution rate D to move to case (6).

Consider the domains

$$\mathcal{D}_5 := \{(s_1^{in}, s_2^{in}, D) \in \mathbb{R}_+^3; \alpha D < \mu_1(s_1^{in}), \alpha D \leq \mu_2^m, \overline{s_2^{in}}(D) > \lambda_2^+(D)\}$$

$$\mathcal{D}_6 := \{(s_1^{in}, s_2^{in}, D) \in \mathbb{R}_+^3; \alpha D < \mu_1(s_1^{in}), \alpha D \leq \mu_2^m, \lambda_2^-(D) < \overline{s_2^{in}}(D) \leq \lambda_2^+(D)\}$$

which are the sets of operating parameters (s_1^{in}, s_2^{in}, D) that correspond to cases (5) and (6) of Proposition 1.

Consider the interval

$$I := (0, \min(\mu_1^m, \mu_2^m)/\alpha)$$

and introduce the functions defined on I :

$$\nu^-(D) := \lambda_1(D) + \lambda_2^-(D), \quad \nu^+(D) := \lambda_1(D) + \lambda_2^+(D), \quad D \in I$$

(that are such that $\nu^- < \nu^+$ on I), which allow to describe the domains \mathcal{D}_5 , \mathcal{D}_6 as follows, using the expression (3) of $\overline{s_2^{in}}(D)$ when $\alpha D < \mu_1(s_1^{in})$.

$$\mathcal{D}_5 = \{(s_1^{in}, s_2^{in}, D) \in \mathbb{R}_+^2 \times [0, \mu_2^m/\alpha]; \alpha D < \mu_1(s_1^{in}); \nu^+(D) < s_1^{in} + s_2^{in}\}$$

$$\mathcal{D}_6 = \{(s_1^{in}, s_2^{in}, D) \in \mathbb{R}_+^2 \times [0, \mu_2^m/\alpha]; \alpha D < \mu_1(s_1^{in}); \nu^-(D) < s_1^{in} + s_2^{in} \leq \nu^+(D)\}$$

Note from expressions (2) and (4) that the functions λ_1 and λ_2^- are increasing, while λ_2^+ is decreasing. The function ν^- is thus increasing. One has also $\nu^-(0) = 0$ and $\nu^-(D) \rightarrow +\infty$ when $D \rightarrow \min(\mu_1^m, \mu_2^m)/\alpha$. One can then define the inverse function

$$\eta^-(s) := (\nu^-)^{-1}(s), \quad s > 0$$

The function ν^+ is not necessarily monotonic but one has $\nu^+(D) \rightarrow +\infty$ when $D \rightarrow 0^+$. Denote

$$s_m := \min_{D \in I} \nu^+(D)$$

and one can define the function

$$\eta^+(s) := \max\{D \in I; \nu^+(D) \leq s\}, \quad s > s_m.$$

Note that $\nu^- < \nu^+$ on I implies that one has $\eta^-(s) > \eta^+(s)$ for any $s > s_m$.

Our main result is the following.

Proposition 2 Consider a triplet (s_1^{in}, s_2^{in}, D) with $s_1^{in} > 0$, $s_2^{in} \geq 0$ and $D > 0$, that do not belong to \mathcal{D}_6 .

(i) For other operating conditions $(s_1^{in}, s_2^{in}, \underline{D})$ with \underline{D} lower than D and sufficiently small, $(s_1^{in}, s_2^{in}, \underline{D})$ belongs to \mathcal{D}_6 .

(ii) If (s_1^{in}, s_2^{in}, D) belongs to \mathcal{D}_5 with the condition

$$\alpha \eta^+(s_1^{in} + s_2^{in}) < \mu_1(s_1^{in}) \quad (7)$$

fulfilled, then any $\bar{D} \in (\eta^+(s_1^{in} + s_2^{in}), \min(\mu_1(s_1^{in})/\alpha, \eta^-(s_1^{in} + s_2^{in})))$ is such that $\bar{D} > D$ and $(s_1^{in}, s_2^{in}, \bar{D})$ belongs to \mathcal{D}_6 .

PROOF. Fix $s_1^{in} > 0$ and $s_2^{in} \geq 0$.

Note first that $\nu^-(0) = 0$ and $\nu^+(0+) = +\infty$ imply that one has $\nu^-(D) < s_1^{in} + s_2^{in} \leq \nu^+(D)$ for $D > 0$ small enough. Therefore, for any $D > 0$, there exists $\underline{D} \in (0, D)$ such that $(s_1^{in}, s_2^{in}, d) \in \mathcal{D}_6$ for any $d \leq \underline{D}$. This shows (i).

Let us now study if it possible to have $(s_1^{in}, s_2^{in}, \bar{D}) \in \mathcal{D}_6$ with $\bar{D} > D$ when $D > 0$ is such that $(s_1^{in}, s_2^{in}, D) \notin \mathcal{D}_6$.

According to Proposition 1, in cases (1), (2) or (3), one has $\alpha D \geq \mu_1(s_1^{in})$ and D has then to be reduced to fulfill the condition $\alpha D < \mu_1(s_1^{in})$ required in case (6).

In case (4), either one has $\alpha D > \mu_2^m$, and \underline{D} has to be reduced to fulfill the condition $\alpha \underline{D} \leq \mu_2^m$ of case (6), or one has $s_2^{in}(D) \leq \lambda_2^-(D)$. This latter situation amounts to write $s_1^{in} + s_2^{in} \leq \nu^-(D)$ and as the function ν^- is increasing, D has again to be reduced to obtain the condition $s_1^{in} + s_2^{in} > \nu^-(D)$ of case (6).

In case (5), one has $s_1^{in} + s_2^{in} > \nu^+(D)$ which implies $D < \eta^+(s_1^{in} + s_2^{in})$ by definition of η^+ . If $\alpha \eta^+(s_1^{in} + s_2^{in}) < \mu_1(s_1^{in})$, then any \bar{D} in the interval $(\eta^+(s_1^{in} + s_2^{in}), \mu_1(s_1^{in})/\alpha)$ verifies $s_1^{in} + s_2^{in} \leq \nu^+(\bar{D})$. If moreover one has $\bar{D} < \eta^-(s_1^{in} + s_2^{in})$ (recall that $\eta^+ < \eta^-$), one guarantees the inequality $s_1^{in} + s_2^{in} < \eta^-(\bar{D})$. This proves the point (ii). \square

The surprising fact, when compared to the usual chemostat model, is that increasing the dilution rate D can bring stability in certain situations given in (ii). Indeed, increasing the dilution rate amounts to reduce the residence time, which is usually a factor of instability. Here, the key point for such a phenomenon to occur relies on the possible non monotonicity of the function ν^+ , which implies that the function η^+ is non identically equal to $\min(\mu_1^m, \mu_2^m)/\alpha$. Let us show that the conditions of case (ii) of Proposition 2 can be really met.

Proposition 3 Assume one has $\mu_2^m \geq \mu_1^m$. Let

$$D_m := \max\{D \in I; \nu^+(D) = s_m\}.$$

(i) Any triplet (s_1^{in}, s_2^{in}, D) such that $s_1^{in} + s_2^{in} > s_m$ and $D > D_m$ with $\nu^+(D) < s_1^{in} + s_2^{in}$ belongs to \mathcal{D}_5 and verifies the inequality (7), provided that s_2^{in} is sufficiently small.

(ii) Any triplet $(s_1^{in}, 0, D)$ that belongs to \mathcal{D}_5 satisfies the inequality (7).

PROOF.

Notice first that when $\mu_2^m \geq \mu_1^m$, μ_1^m is necessarily finite and one has $I = (0, \mu_1^m/\alpha)$.

Take any $s > s_m$ and denote $\tilde{D} = \eta^+(s)$. For any $D > D_m$ in I such that $\nu^+(D) < s$, one has

$$\lambda_1(D) < s - \lambda_2^+(D).$$

As $D < \tilde{D}$ and λ_2^+ is decreasing, one has also

$$\lambda_1(D) < s - \lambda_2^+(\tilde{D}). \quad (8)$$

Consider now any $s_2^{in} < \min(s, \lambda_2^+(\tilde{D}))$ and take $s_1^{in} = s - s_2^{in}$. For this choice of s_1^{in} and s_2^{in} , inequality (8) gives

$$\lambda_1(D) < s_1^{in}$$

(along with $\nu^+(D) < s_1^{in} + s_2^{in}$). As the interval I is equal to $(0, \mu_1^m/\alpha)$ and the function μ_1 is increasing, having $\lambda_1(D) < s_1^{in}$ is equivalent to have $\alpha D < \mu_1(s_1^{in})$. This shows that the triplet (s_1^{in}, s_2^{in}, D) belongs to \mathcal{D}_5 (notice that one has necessarily $\alpha D < \mu_2^m$ as $\mu_1^m \leq \mu_2^m$).

For $D = \tilde{D}$, one has $\nu^+(\tilde{D}) = s$. In the same manner, one obtains $\lambda_1(\tilde{D}) < s_1^{in}$ for the former choice of s_1^{in} and s_2^{in} , or equivalently $\alpha\tilde{D} < \mu_1(s_1^{in})$. This shows that the inequality

$$\alpha\eta^+(s_1^{in} + s_2^{in}) < \mu_1(s_1^{in})$$

is necessarily fulfilled.

For the particular case $s_2^{in} = 0$, note that $\nu^+(D) < s_1^{in}$ implies $\lambda_1(D) < s_1^{in}$ which, in turns, implies $\alpha D < \mu_1(s_1^{in})$. From the definition of ν^+ , this shows that the inequality $\alpha\eta^+(s_1^{in}) < \mu_1(s_1^{in})$ is verified. \square

4 Numerical illustrations

4.1 Simulations

Typical instances of functions that fulfill Assumption 1 are given by the Monod expression for the first reaction

$$\mu_1(s_1) = \frac{\mu_1^m s_1}{K_1 + s_1}. \quad (9)$$

and the Haldane one for the second

$$\mu_2(s_2) = \frac{\bar{\mu}_2 s_2}{K_2 + s_2 + \frac{s_2^2}{K_i}} \quad (10)$$

for which one has

$$\hat{s}_2 = \sqrt{K_2 K_i}.$$

Then, the break even concentrations defined in Section 2 have the expressions

$$\lambda_1(D) = \frac{\alpha D K_1}{\mu_1^m - \alpha D}, \quad \alpha D < \mu_1^m$$

for the Monod function (9), and for the Haldane function (10)

$$\lambda_2^\pm(D) = \frac{\bar{\mu}_2 - \alpha D \pm \sqrt{(\bar{\mu}_2 - \alpha D)^2 - 4(\alpha D)^2 \frac{K_2}{K_i}}}{2 \frac{\alpha D}{K_i}}, \quad \alpha D \leq \mu_2^m$$

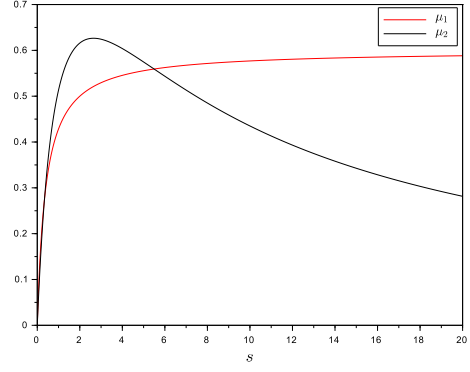
Figure 2 gives the values of the parameters chosen for the numerical computation, along with the graphs of the corresponding functions μ_1 , μ_2 . The numerical values of the parameters were chosen such that the graphical representations be very clear and the phenomenon very well put in evidence. We will come back on this point in the discussion at the end of this section but the phenomenon appears for several parameter sets reported in the literature even if it may be less obvious and more difficult to represent graphically (cf. for instance [14]) as well as for more complicated models, (cf. [7, 20] for example).

For these values, one has $\hat{s}_2 \simeq 2.646$ and $\mu_2^m \simeq 0.626$. So, we are in the case $\mu_2^m > \mu_1^m$ of Proposition 3.

Figure 3 gives the graphs of the associated break-even concentrations λ_1 , λ_2^\pm and the functions ν^\pm .

μ_1^m	K_1	$\bar{\mu}_2$	K_2	K_i	α
0.6	0.4	1.1	1	7	0.7

(a) Parameters values.



(b) Graphs of μ_1 and μ_2 .

Fig. 2.

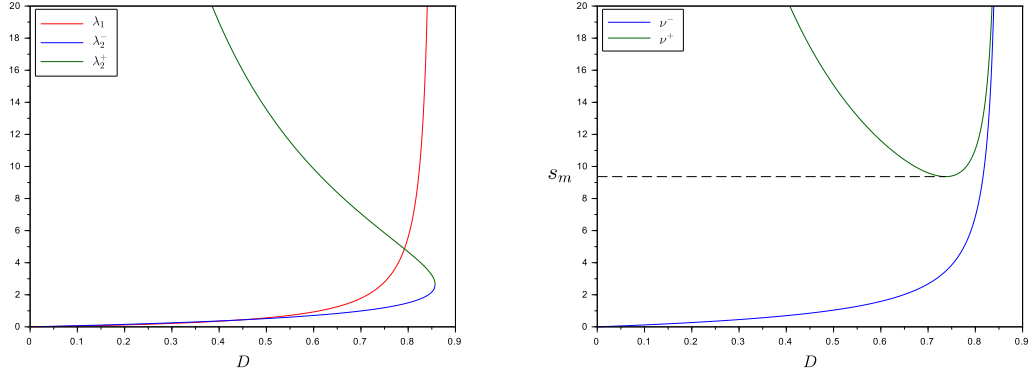


Fig. 3. Graphs of the functions λ_i^\pm (left) and $\nu^\pm = \lambda_1 + \lambda_2^\pm$ (right).

Remind that λ_1 and λ_2^- are increasing while λ_2^+ is decreasing. The function ν^+ is always above ν^- (which is increasing) and ν^+ tends to $+\infty$ on the boundary of the interval $I = (0, \mu_1^m/\alpha)$ when $\mu_1^m \leq \mu_2^m$.

As it is not always easy to grasp domains in \mathbb{R}^3 , we fix values of s_2^{in} and depict the cross-sections of the domains \mathcal{D}_5 , \mathcal{D}_6 in the (s_1^{in}, D) plane. For a fixed value of s_2^{in} , these cross-sections are

$$\mathcal{C}_5(s_2^{in}) := \{(s_1^{in}, D) \in \mathbb{R}_+ \times I, \alpha D < \mu_1(s_1^{in}); \nu^+(D) < s_1^{in} + s_2^{in}\}$$

$$\mathcal{C}_6(s_2^{in}) := \{((s_1^{in}, D) \in \mathbb{R}_+ \times I, \alpha D < \mu_1(s_1^{in}); \nu^-(D) < s_1^{in} + s_2^{in} \leq \nu^+(D)\}$$

It can be simply interpreted in terms of intersections of epigraphs or hypographs of the functions λ_1 , $\nu^+ - s_2^{in}$ and $\nu^- - s_2^{in}$ in the (D, s_1^{in}) symmetric

plane:

$$\mathcal{C}_5(s_2^{in}) := \{s_1^{in} > \lambda_1(D)\} \cup \{s_1^{in} > \nu^+(D) - s_2^{in}\}$$

$$\mathcal{C}_6(s_2^{in}) := \{s_1^{in} > \lambda_1(D)\} \cup \{s_1^{in} \leq \nu^+(D) - s_2^{in}\} \cup \{s_1^{in} > \nu^-(D) - s_2^{in}\}$$

Accordingly to Proposition 2, the complementary of $\mathcal{C}_5(s_2^{in}) \cup \mathcal{C}_6(s_2^{in})$ in the domain $\{(s_1^{in}, D) \in \mathbb{R}_+ \times I ; \alpha D < \mu_1(s_1^{in})\}$ corresponds to case (4) and the complementary $\{(s_1^{in}, D) \in \mathbb{R}_+^2 ; \alpha D \geq \mu_1(s_1^{in})\}$ is covered by cases (1), (2) and (3).

In Figure 4, one can see that for $s_2^{in} = 0$, \mathcal{C}_5 and \mathcal{C}_6 cover almost but not all the domain $\{\alpha D < \mu_1(s_1^{in})\}$ (which is below the red curve), and that it is always possible to reach the domain \mathcal{C}_6 (in green) from \mathcal{C}_5 (in pink) by increasing D (for fixed s_1^{in}), in accordance with Proposition 3. The red curve, which is the graph of the function μ_1/α , is above the domain \mathcal{C}_5 .

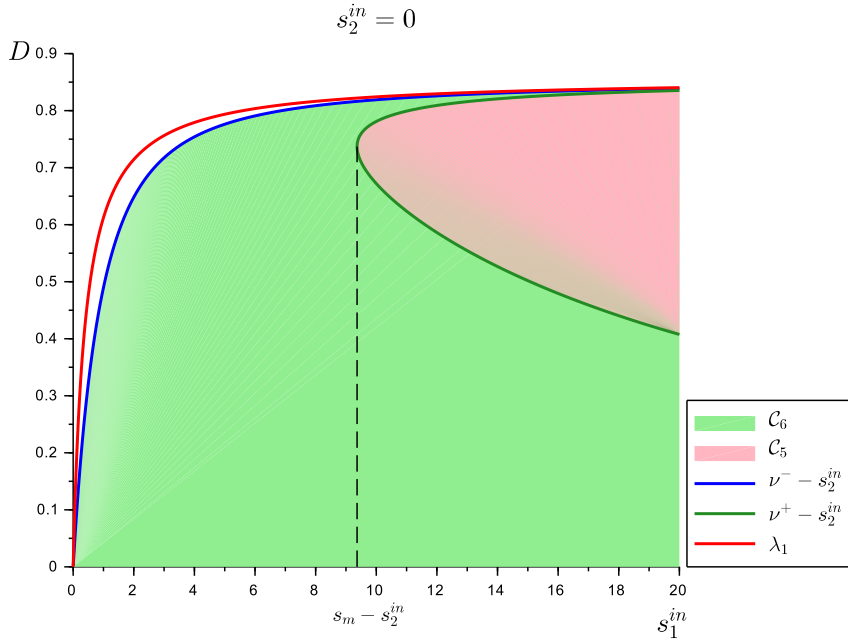


Fig. 4. Cross-sections of the domains \mathcal{D}_5 and \mathcal{D}_6 for $s_2^{in} = 0$. From any operating point $(s_1^{in}, D) \in \mathcal{C}_5$ it is possible to reach \mathcal{C}_6 by simply increasing D .

For $s_2^{in} = 2$ or $s_2^{in} = 5$, \mathcal{C}_5 and \mathcal{C}_6 cover all the domain $\{D < \mu_1(s_1^{in})/\alpha\}$ and the graph of the red curve touches the boundary \mathcal{C}_5 (see Figure 5). However, it is still possible to reach \mathcal{C}_6 from \mathcal{C}_5 by increasing D only if s_1^{in} is close enough to the value $s_m - s_2^{in}$ (remind that s_m is the minimum of the function ν^+).

Increasing the values of s_2^{in} slides further the cross-section \mathcal{C}_5 to the left on the (s_1^{in}, D) plane and it is no longer possible to reach \mathcal{C}_6 from \mathcal{C}_5 by simply

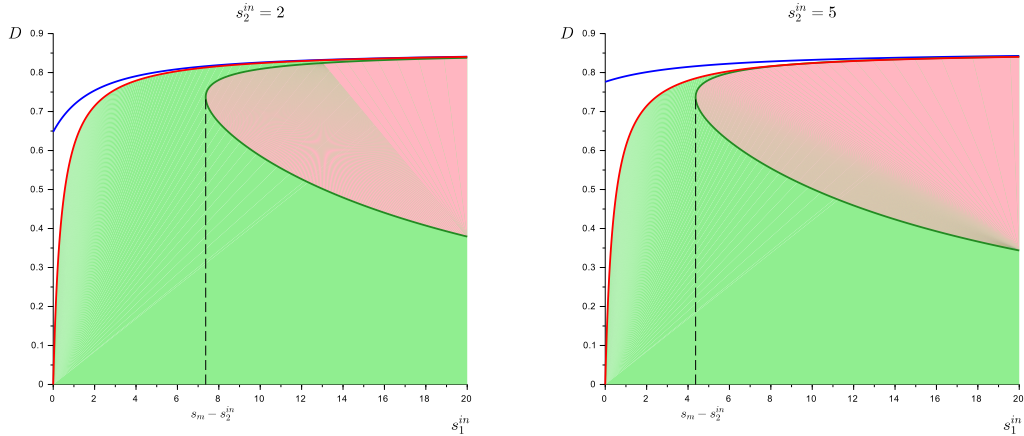


Fig. 5. Cross-sections of the domains \mathcal{D}_5 and \mathcal{D}_6 for $s_2^{in} = 2$ and $s_2^{in} = 5$. From an operating point $(s_1^{in}, D) \in \mathcal{C}_5$ with s_1^{in} not too far from $s_m - s_2^{in}$, it is possible to reach \mathcal{C}_6 by simply increasing D .

increasing D (see Figure 6), exactly when the extreme point $(s_m - s_2^{in}, D_m)$ of \mathcal{C}_5 does no longer lie in the domain $\{\alpha D < \mu_1(s_1^{in})\}$ (*i.e.* when it is no longer located below the red curve). Then, the only way to stabilize the system playing only with the dilution rate D is to decrease its value such that (s_1^{in}, D) is below the green curve (which is the graph of the function $\nu^+ - s_2^{in}$).

Notice that this interesting property of two-step processes was already visible in certain figures of some papers of the literature, notably in relation to the analysis of the anaerobic digestion process (cf. for instance the Figure 4 of the paper by Sbarciog *et al.*, 2010, [14]). However, the property was not underlined in the paper as a way to stabilize the system. It should be noticed that this property obviously appears in more complex models. In [7], which studied a model of the anaerobic digestion of micro-algae, this property was highlighted. In particular, when comparing the two models of the anaerobic digestion initially proposed in [4] and [5], it was first noticed that the inhibition coefficient identified in the first model, ([4]) was too large to play a role in the system dynamics (recall that having a large inhibition coefficient in the Haldane function amounts to considering a Monod kinetics). Then, in modifying this coefficient (increasing the inhibition of the second step kinetics in decreasing the value of the inhibition coefficient in the Haldane kinetics), it was possible to show that the region in which the biogas is maximum exhibits a bi-stability. Comparing these results with those obtained when studying the second model (from [5]) yielded to plot the Figure 11 of [7] where this property is visible (but not further discussed). Finally, this property has been described in [13] for two-step biological systems with density-dependent kinetics in the first step, but again without giving any condition to test it nor proposing a control strategy to take advantage of it. Here we give sufficient conditions that can easily be tested for the phenomenon to appear.

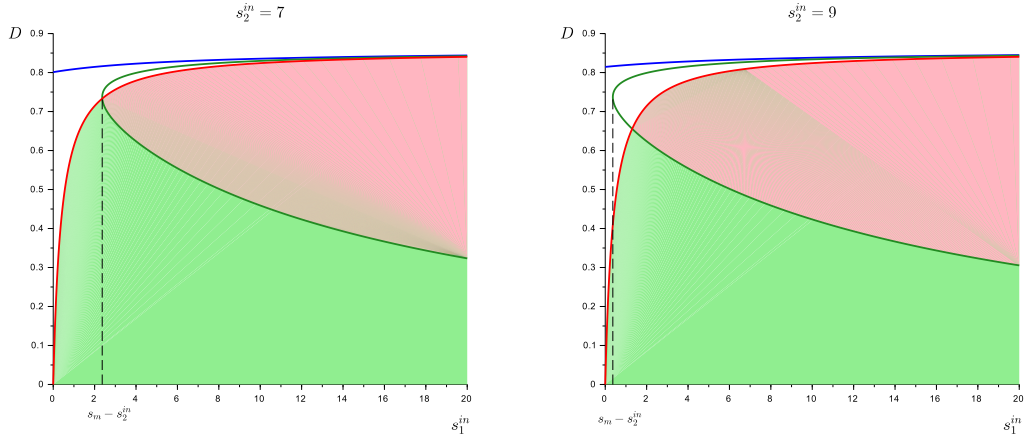


Fig. 6. Cross-sections of the domains \mathcal{D}_5 and \mathcal{D}_6 for $s_2^{in} = 7$ and $s_2^{in} = 9$. From any operating point $(s_1^{in}, D) \in \mathcal{C}_5$ it is not possible to reach \mathcal{C}_6 by simply increasing D .

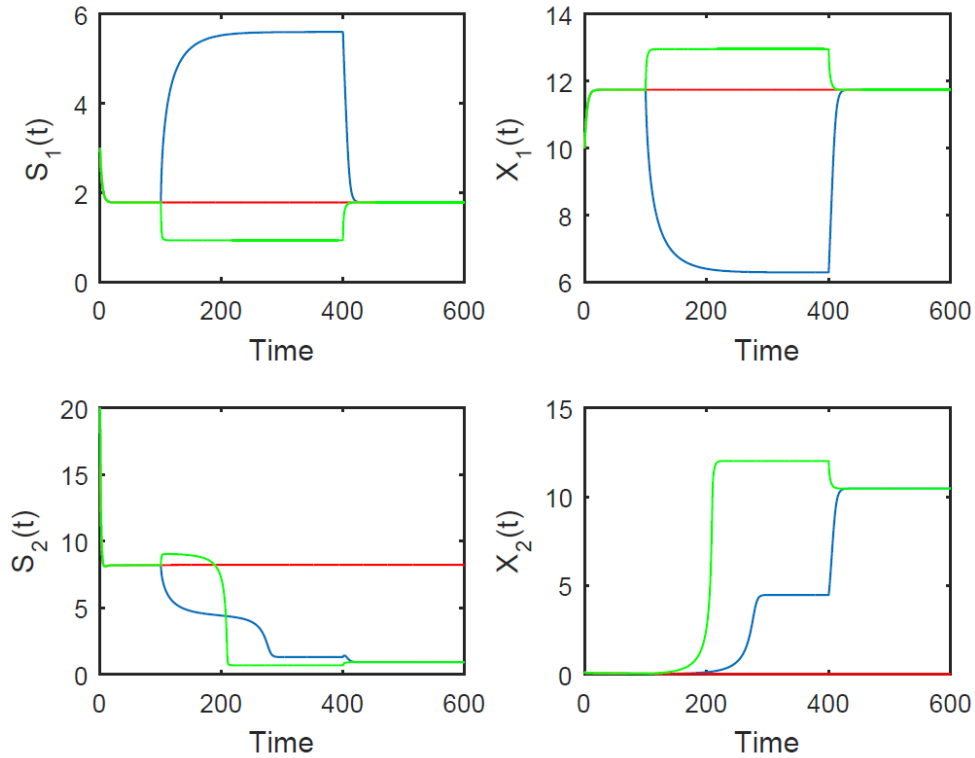


Fig. 7. Dynamical simulation of the two-step system. The trajectories of the system with a constant dilution rate ($D = 0.7$) are plotted in red: the washout of X_2 is globally attracting. In blue, with the same initial conditions, the dilution rate is changed to 0.8 at $t = 100$ and then switched back to $D = 0.7$ at $t = 400$: the system is now globally attracted by a positive steady state. In green, again for the same initial conditions, the trajectories are plotted when the classical strategy is used: the dilution rate is changed to 0.6 at $t = 100$ and then switched back to $D = 0.7$ at $t = 400$.

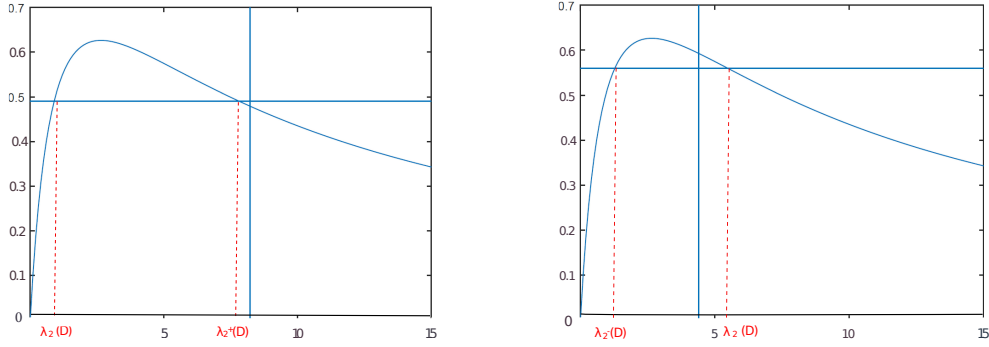


Fig. 8. Graph of μ_2 with horizontal lines representing the value αD and the vertical ones $s_2 = \overline{s_2^{in}}(D)$ for $D = 0.7$ (left) and $D = 0.8$ (right).

To illustrate the approach, we simulated the two-step system with the parameter values considered here-above over a time $T = 600$. For the initial conditions $X_1(0) = 10$, $S_1(0) = 3$, $X_2(0) = 0.1$, $S_2(0) = 20$ and for a constant dilution rate $D = 0.7$, the results are plotted in red in Figure 7. It can be seen that X_2 is washed out. We can check in the first picture of Figure 8 that the system exhibits bi-stability for this value of D since $\overline{s_2^{in}}(D)$ is larger than λ_2^+ . Let us apply our control strategy: for the same initial conditions, the system is simulated again but, at $t = 100$, D is increased from 0.7 to 0.8 and then switched back to 0.7 at $t = 400$. It can be seen in the second picture of Figure 8 that for $D = 0.8$, the only positive equilibrium is the one for which $s_2 = \lambda_2^-$ (λ_2^+ being this time larger than $\overline{s_2^{in}}(D)$ and is thus no longer a possible value for s_2 at steady-state). The counter-intuitive result is that X_2 will not finally be washed out while it may become very small during the transient. In the proposed simulations however, it was checked that the minimum of X_2 over time is 0.017, which sounds acceptable from a biological point of view. Finally, the performances of the new strategy may be compared to more classical ones. To do so, we consider an additional simulation that consists in simulating the system under the same conditions but instead of increasing the dilution rate at $t = 100$, we decrease it at $D = 0.6$, before switching back it at $D = 0.7$ at $t = 400$. The value $D = 0.6$ has been chosen because it is the symmetric one of $D = 0.8$ with respect to $D = 0.7$: the corresponding steady states - both in \mathcal{C}_6 are practically at the same distance from \mathcal{C}_5 . Thus both strategies can be said to be comparable in terms of stability. The reader may check in Figure 4 that with $D = 0.6$ the system is indeed operating in \mathcal{C}_6). The corresponding trajectories are plotted in green in Figure 8. The index performances that are compared are the absolute quantity of matter processed (that is $\int_0^T D(\tau)S_1^{in}d\tau$) and the output concentrations (pollutants) S_1 and S_2 over 500 units of time. For the classical strategy, the total matter processed over this time period is 3200 while it is equal to 3800 for the new proposed strategy. As explained above, the actual strategy allows to process much more matter than the classical one. The price to pay is the washout risk taken during the

transient. Concerning the output substrate concentrations, since the new approach considers a higher dilution rate, these index performances cannot be better than with the classical approach. It may be seen in Figure 7 that the index is indeed significantly degraded for S_1 . However, note that this takes place only during the transient and that it is almost equivalent for S_2 : we have treated much more matter with the new strategy than with the classical one while the performance in terms of treatment only affected transiently one substrate.

4.2 About practical implementation of the proposed control strategy

The proposed strategy consists in decreasing the residence time (in increasing the dilution rate) and not increasing it as usually done to stabilize bioprocesses. This has some practical advantages: it allows to treat a larger quantity of matter and for industrial plants that impose a minimal flow rate to be processed, it does not require any upstream storage. Of course, increasing the residence time increases the output concentration at steady-state, but once close to the nominal steady-state one may reduce the flow rate to its nominal value.

For a number of reasons, it may appear to be risky to apply this control strategy on a real plant. Indeed, it should be noted that the range of dilution rate allowing to globally stabilize the process in increasing it (going from \mathcal{C}_5 to \mathcal{C}_6 in Fig 3 or 4) is quite narrow although the model parameters were chosen to highlight the phenomenon. The property which is highlighted is the consequence of model parameter values and conditions under which the process is operated (values of inputs: the dilution rate and the input substrate concentration). We take advantage of this property to propose a way to globally stabilize the system but - unless the exact model of the system be known - the value of the dilution rate to apply to effectively stabilize the system is unknown. In other words, there is not an adaptive strategy. In practice, there is obviously a non negligible risk to not increase the dilution rate enough (resp. a little bit too much) such that the process be in a situation where it continues towards the washout - it remains in \mathcal{C}_5 (resp. the washout is the only global stable steady state - it directly goes over \mathcal{C}_6). In other words, the study of the robustness of the control with respect to model parameters and inputs should be carefully investigated before testing it in practice. From Figures 4 or 5, it may be seen that this robustness is all the greater as S_1^{in} remains close to $S_m - S_2^{in}$ (while being greater) where S_m is the minimum of ν^+ . To avoid any problem, some implementation precautions could be taken. For instance, some tolerance index such as that one proposed in [3] in revisiting the index initially proposed by Hess and Bernard (*cf.* [24]), could be used. Such tolerance index was precisely proposed to estimate the distance between the actual operating

conditions and the washout. Of course additional work would be needed to be able to estimate on-line such index but for sure its monitoring would greatly help to manage the process within the narrow region of interest. Another possibility would be to adapt the strategy initially proposed by Steyer *et al.*, 1999 for the optimization of the anaerobic digestion process, *cf.* [26]. This strategy, which was further shown to be optimal with respect to a time criterion (*cf.* [25]), is based on a ‘dialogue’ between the user and the process. Initially, it is supposed that an overproduction of biogas should be observed after a shock load. If not, it means that inter-metabolites have accumulated and the process is operating in a bad manner. If yes, the process is working well and the dilution rate can be increased. Here, the idea would be adapted (imagine the system goes towards washout). Instead of decreasing the dilution rate, it would be increased slightly. Monitoring carefully the response of the system to this change would certainly help us in applying such a counter-intuitive control strategy. Finally, an relevant challenge would be to find a robust control feedback that would stabilize the system under the constraint that the control remains larger or equal to its nominal value, despite some uncertainties on the knowledge of the growth functions. In such a way we should be able to synthesis the right control in \mathcal{C}_6 . The adaptive character of such a feedback, which is already used to stabilize the model of the classical chemostat with non-monotonic growth, for example using a PI (*cf.* [9], the integral term allowing to learn the nominal value of D necessary to maintain the system at a desired equilibrium state), would make the strategy robust both with respect to the model and with respect to disturbances. This question is beyond the present work and part of perspectives.

5 Conclusion

This study reveals the role played by the sum of the break-even concentrations, as the function $D \mapsto \lambda_1(D) + \lambda_2^+(D)$, in the counter-intuitive phenomenon of increasing the dilution rate to stabilize a two-steps bio-process model. More precisely, we show that when this function is non-monotonic on its domain, this phenomenon occurs provided that the input concentration s_2^{in} of substrate of the second reaction is null or not too large. This result provides a new way to stabilize such processes in certain situations, without increasing the residence time, as it is often done which may be penalizing in an industrial context.

Appendix

We recall here the classical results about the chemostat model

$$\begin{cases} \dot{x} = \mu(s)x - \alpha Dx \\ \dot{s} = -\mu(s)x + D(s^{in} - s) \end{cases} \quad (11)$$

when μ is a monotonic or non-monotonic function.

Proposition 4 *Assume that the function μ is increasing on $(0, s^{in})$ and define the break-even concentration $\lambda(D)$ such that*

$$\mu(\lambda(D)) = \alpha D, \quad \alpha D \in (0, \mu(s^{in}))$$

- *When $\alpha D \geq \mu(s^{in})$, the system (11) has an unique equilibrium $E^0 := (0, s^{in})$ ("wash-out"), which is moreover globally asymptotically stable on \mathbb{R}_+^2 .*
- *When $\alpha D < \mu(s^{in})$, the system (11) admits an unique positive equilibrium $E^+ := ((s^{in} - \lambda(D))/\alpha, \lambda(D))$ (in addition to the equilibrium E^0), which is moreover globally asymptotically stable on the domain $\mathbb{R}_+^* \times \mathbb{R}_+$.*

Proposition 5 *Assume that there exists $\hat{s} \in (0, s^{in})$ such that the function μ is increasing on $(0, \hat{s})$ and decreasing on (\hat{s}, s^{in}) . Define the break-even concentrations $\lambda^-(D)$, $\lambda^+(D)$ as follows*

$$\begin{aligned} \lambda^-(D) &= \min\{s \in [0, \hat{s}] ; \mu(s) \geq \alpha D\}, \quad \alpha D \in [0, \mu(\hat{s})] \\ \lambda^+(D) &= \max\{s \in [\hat{s}, s^{in}] ; \mu(s) \geq \alpha D\}, \quad \alpha D \in [\mu(s^{in}), \mu(\hat{s})] \end{aligned}$$

- *If $\alpha D > \mu(\hat{s})$, the system (11) has the unique equilibrium $E^0 := (0, s^{in})$, which is globally asymptotically stable on \mathbb{R}_+^2 .*
- *If $\alpha D < \mu(s^{in})$, the system (11) admits an unique positive equilibrium $E^- := ((s^{in} - \lambda^-(D))/\alpha, \lambda^-(D))$ which is globally asymptotically stable on $\mathbb{R}_+^* \times \mathbb{R}_+$.*
- *If $\alpha D \in [\mu(s^{in}), \mu(\hat{s})]$, the system (11) presents a bi-stability between E^- and E^0 . From any initial condition in $\mathbb{R}_+^* \times \mathbb{R}_+$ excepted on a set of null measure, the solution converges asymptotically to E^- or E^0 .*

Acknowledgments

The work has been achieved in the framework of the PHC program 'TOURNESOL' 2018-19 between France and Belgium-Wallonia. The authors are very grateful to Professor Tewfik Sari for fruitful discussions.

References

- [1] G. Bastin, D. Dochain (1990) *On-line Estimation and Adaptive Control of Bioreactors*, Elsevier.
- [2] D.J. Batstone, J. Keller, I. Angelidaki, S.V. Kalyzhnyi, S.G. Pavlostathis, A. Rozzi, W.T.M. Sanders, H. Siegrist, V.A. Vavilin (2002) The Iwa Anaerobic Digestion Model No 1 (ADM1). *Water Science and Technology* 45, 65-73.
- [3] B. Benyahia, T. Sari, B. Cherki, J. Harmand (2012) Bifurcation and stability analysis of a two step model for monitoring anaerobic digestion processes. *J. Process Control* 22, 1008-1019.
- [4] O. Bernard, Z. Hadj-Sadock, D. Dochain, A. Genovesi, J.-P. Steyer (2001) Dynamical model development and parameter identification for an anaerobic wastewater treatment process. *Biotechnology and Bioengineering* 75, 424-438.
- [5] F. Mairet, O. Bernard, E. Cameron, M. Ras, L. Lardon, J.P. Steyer, B. Chachuat (2011) Three-reaction model for the anaerobic digestion of microalgae, *Biotechnology and Bioengineering* 109, 415-429.
- [6] J. Harmand, C. Lobry, A. Rapaport, T. Sari (2017) *The Chemostat: Mathematical Theory of Microorganism Cultures*, John Wiley & Sons.
- [7] Z. Khedim, B. Benyahia, B. Cherki, T. Sari, J. Harmand (2018) Effect of control parameters on biogas production during the anaerobic digestion of protein-rich substrates, *Applied Mathematical Modelling* 61, 351-376.
- [8] A. Rapaport, J. Harmand (2002) Robust regulation of a class of partially observed nonlinear continuous bioreactors. *Journal of Process Control* 12, 291-302.
- [9] A. Schaum, J. Alvarez, T. Lopez-Arenas (2012) Saturated PI control of continuous bioreactors with Haldane kinetics, *Chemical Engineering Science* 68 (1), 520-529.
- [10] H.L. Smith, P. Waltman (1995) *The theory of the chemostat : dynamics of microbial competition*, Cambridge university press.
- [11] I. Ramirez, A. Mottet, H. Carrère, S. Déléris, F. Vedrenne, J.P. Steyer (2009) Modified ADM1 disintegration/hydrolysis structures for modeling batch thermophilic anaerobic digestion of thermally pretreated waste activated sludge, *Water Research*, 43 (14), 3479-3492.
- [12] P.J. Reilly (1974) Stability of commensalistic systems, *Biotechnology and Bioengineering* 16, 1373-1392.
- [13] M. Hanaki, J. Harmand, Z. Mghazli, T. Sari, A. Rapaport, P. Ugalde, Mathematical study of a two-stage anaerobic model when the hydrolysis is the limiting step, preprint hal.archives-ouvertes.fr/hal-02531141.
- [14] M. Sbarciog, M. Loccufier, E. Noldus (2010) Determination of appropriate operating strategies for anaerobic digestion systems, *Biochemical Engineering Journal* 51 (3), 180-188.
- [15] T. Sari, B. Benyahia (2020) The operating diagram for a two-step anaerobic digestion model, preprint

hal.archives-ouvertes.fr/hal-02557464.

- [16] T. Sari, J. Harmand (2016) A model of a syntrophic relationship between two microbial species in a chemostat including maintenance, *Mathematical Biosciences* 275, 1-9.
- [17] B. Satishkumar, M. Chidambaram (1999) Control of unstable bioreactor using fuzzy-tuned PI controller, *Bioprocess Engineering* 20, 127-132.
- [18] G. Stephanopoulos (1981) The dynamic of commensalism, *Biotechnology and Bioengineering* 23, 2243-2255.
- [19] V.A. Vavilin, B. Fernandez, J.Palatsi, X.Floutats (2008) Hydrolysis kinetics in anaerobic degradation of particulate organic material: An overview, *Waste Management* 28, 939-951.
- [20] E. Volcke, M. Sbarciog, E.J.L. Noldus, B. De Baets, M. Loccupier (2010) Steady-state multiplicity of two-step biological conversion systems with general kinetics, *Mathematical Biosciences* 228, 160-170.
- [21] M.J. Wade, J. Harmand, B. Benyahia, T. Bouchez, S. Chailou, B. Cloez, J-J. Godon, B. Moussa Boudjmaa, A. Rapaport, T. Sari, R. Arditi, C. Lobry (2016). Perspectives in mathematical modelling for microbial ecology, *Ecological Modelling* 321, 64-74.
- [22] M. Weeder mann, G. Seo, G. Wolkowicz (2013) Mathematical Model of Anaerobic Digestion in a Chemostat: Effects of Syntrophy and Inhibition, *Journal of Biological Dynamics* 7, 59-85.
- [23] M. Weeder mann, G. Wolkowicz, J. Sasara (2015) Optimal biogas production in a model for anaerobic digestion, *Nonlinear Dynamics* 81, 1097-1112.
- [24] J. Hess, O. Bernard (2008) Design and Study of a risk management criterion for an unstable anaerobic wastewater treatment process, *Journal of Process Control* 18, 71-79.
- [25] A. Ghouali, T. Sari, J. Harmand (2015) Maximizing biogas production from the anaerobic digestion, *Journal of Process Control*, 36, 79-86.
- [26] J.P. Steyer, P. Buffière, D. Rolland, R. Moletta (1999) Advanced control of anaerobic digestion processes through disturbances monitoring, *Water Research* 33 (9), 2059-2068.